

# CARMENES: Calar Alto high-Resolution search for M dwarfs with Exo-earths with Near-infrared and optical Echelle Spectrographs

A. Quirrenbach<sup>a</sup>, P.J. Amado<sup>b</sup>, H. Mandel<sup>a</sup>, J.A. Caballero<sup>c</sup>, R. Mundt<sup>d</sup>, I. Ribas<sup>e</sup>,  
A. Reiners<sup>f</sup>, M. Abril<sup>b</sup>, J. Aceituno<sup>g</sup>, C. Afonso<sup>d</sup>, D. Barrado y Navascués<sup>g</sup>, J.L. Bean<sup>f</sup>,  
V.J.S. Béjar<sup>h</sup>, S. Becerril<sup>b</sup>, A. Böhm<sup>d</sup>, M.C. Cárdenas<sup>b</sup>, A. Claret<sup>b</sup>, J. Colomé<sup>e</sup>, L.P. Costillo<sup>b</sup>,  
S. Dreizler<sup>f</sup>, M. Fernández<sup>b</sup>, X. Francisco<sup>e</sup>, D. Galadí<sup>g</sup>, R. Garrido<sup>b</sup>, J.I. González Hernández<sup>h</sup>,  
J. Guàrdia<sup>e</sup>, E.W. Guenther<sup>i</sup>, J. Gutiérrez-Soto<sup>b</sup>, V. Joergens<sup>d</sup>, A.P. Hatzes<sup>i</sup>, J. Helmling<sup>g</sup>,  
T. Henning<sup>d</sup>, E. Herrero<sup>e</sup>, M. Kürster<sup>d</sup>, W. Laun<sup>d</sup>, R. Lenzen<sup>d</sup>, U. Mall<sup>d</sup>, E.L. Martín<sup>c</sup>,  
S. Martín-Ruiz<sup>b</sup>, E. Mirabet<sup>b</sup>, D. Montes<sup>j</sup>, J.C. Morales<sup>e</sup>, R. Morales Muñoz<sup>b</sup>, A. Moya<sup>c</sup>,  
V. Naranjo<sup>d</sup>, O. Rabaza<sup>b</sup>, A. Ramón<sup>b</sup>, R. Rebolo<sup>h</sup>, S. Reffert<sup>a</sup>, F. Rodler<sup>h</sup>, E. Rodríguez<sup>b</sup>,  
A. Rodríguez Trinidad<sup>b</sup>, R.R. Rohloff<sup>d</sup>, M.A. Sánchez Carrasco<sup>b</sup>, C. Schmidt<sup>f</sup>, W. Seifert<sup>a</sup>,  
J. Setiawan<sup>d</sup>, E. Solano<sup>c</sup>, O. Stahl<sup>a</sup>, C. Storz<sup>d</sup>, J.C. Suárez<sup>b</sup>, U. Thiele<sup>g</sup>, K. Wagner<sup>d</sup>,  
G. Wiedemann<sup>k</sup>, M.R. Zapatero Osorio<sup>c</sup>, C. del Burgo<sup>l</sup>, E. Sánchez-Blanco<sup>b</sup>, and W. Xu<sup>m</sup>

<sup>a</sup>Landessternwarte, ZAH, Königstuhl 12, D-69117 Heidelberg, Germany;

<sup>b</sup>Instituto de Astrofísica de Andalucía (CSIC), Glorieta de la Astronomía s/n, E-18008 Granada, Spain;

<sup>c</sup>Centro de Astrobiología (CSIC-INTA), Carretera de Ajalvir km 4, E-28850 Torrejón de Ardoz, Madrid, Spain;

<sup>d</sup>Max-Planck-Institut für Astronomie, Königstuhl 17, D-69117 Heidelberg, Germany;

<sup>e</sup>Instut de Ciències de l'Espai (CSIC-IEEC), Campus UAB, Facultat Ciències, Torre C5 - parell - 2a planta, E-08193 Bellaterra, Barcelona, Spain;

<sup>f</sup>Institut für Astrophysik (GAU), Friedrich-Hund-Platz 1, D-37077 Göttingen, Germany;

<sup>g</sup>Calar Alto Observatory (MPG-CSIC), Centro Astronómico Hispano-Alemán, Jesús Durbán Remón, 2-2, E-04004 Almería, Spain;

<sup>h</sup>Instituto de Astrofísica de Canarias, Vía Láctea s/n, E-38205 La Laguna, Tenerife, Spain;

<sup>i</sup>Thüringer Landessternwarte Tautenburg, Sternwarte 5, D-07778 Tautenburg, Germany;

<sup>j</sup>Departamento de Astrofísica, Facultad de Física, Universidad Complutense de Madrid, E-28040 Madrid, Spain;

<sup>k</sup>Hamburger Sternwarte, Gojenbergsweg 112, D-21029 Hamburg, Germany;

<sup>l</sup>UNINOVA-CA3, Campus da Caparica, Quinta da Torre, Monte de Caparica 2825-149, Caparica, Portugal;

<sup>m</sup>Wenli Xu Optical System Engineering, Kirchenstr. 6, D-74937 Spechbach, Germany

## ABSTRACT

CARMENES (Calar Alto high-Resolution search for M dwarfs with Exo-earths with Near-infrared and optical Echelle Spectrographs) is a next-generation instrument to be built for the 3.5 m telescope at the Calar Alto Observatory by a consortium of Spanish and German institutions. Conducting a five-year exoplanet survey targeting  $\sim 300$  M stars with the completed instrument is an integral part of the project. The CARMENES instrument consists of two separate spectrographs covering the wavelength range from 0.52 to 1.7  $\mu\text{m}$  at a spectral resolution of  $R = 85,000$ , fed by fibers from the Cassegrain focus of the telescope. The spectrographs are housed in a temperature-stabilized environment in vacuum tanks, to enable a 1 m/s radial velocity precision employing a simultaneous ThAr calibration.

**Keywords:** Spectrographs, Optical Instrumentation, Near-Infrared Instrumentation, Extrasolar Planets, M Dwarfs

## 1. INTRODUCTION

Exoplanet research has made enormous progress over the past decade. After the first report of an exoplanet discovered around a “normal” star (Mayor & Queloz 1995), new announcements have been arriving at an ever-increasing pace. Today, over 450 exoplanets are known, with most of the discoveries coming from high-precision radial velocity measurements and a significant number also from photometric transit observations.

Two main lines of development are now taking shape. One is the use of transit spectrophotometry techniques in the visible or IR to characterize the properties of exoplanets, including the physical parameters and chemical composition of their atmospheres (Knutson et al. 2007, Tinetti et al. 2007, Swain et al. 2008). Another one is to push the detection limits of radial velocity searches to planets of lower masses, entering the domain of potentially terrestrial planets, i.e.,  $M_p < 10 M_\oplus$  (Mayor & Udry 2008). An ultimate goal in exoplanet research is the combination of these two paths to find and characterize Earth analogs. This is a challenge that is still beyond the reach of current technology.

The radial velocity amplitude  $K_p$  of a planetary signal is given by

$$K_p = 0.0895 a^{-1/2} M_\star^{-1/2} M_p \sin i \quad , \quad (1)$$

with  $K_p$  in  $\text{m s}^{-1}$ ,  $M_p$  in Earth masses,  $M_\star$  in Solar masses, and  $a$  in AU. Thus, an Earth-mass planet around a Solar-type star produces a radial velocity signal of only  $9 \text{ cm s}^{-1}$ , which is out of the reach of the most precise spectrographs today, reaching accuracies of about  $1 \text{ m s}^{-1}$  (Udry et al. 2007, Mayor et al. 2009a, 2009b) – although claims have been made of rms residuals around  $0.2 \text{ m s}^{-1}$  (Lovis et al. 2006). As can be seen from Eqn. 1, for a given planet mass, the radial velocity amplitude increases with decreasing stellar mass. Therefore, exoplanets around low-mass stars are an obvious choice to reach down to the terrestrial planet range. Indeed, this has already been exploited by spectrographs in the visible (HARPS, HIRES), and low-mass planets (so-called super-Earths with masses between 2 and  $10 M_\oplus$ ) have already been found around some early M-type stars. However, the faintness of the targets and the intrinsic stellar jitter limit the ability to detect planets around even lower-mass stars. Another way to increase the planetary signal is to focus on short orbital distances, and correspondingly short periods. Such short distances usually mean heavily irradiated planets and high planet temperatures. For low-mass stars, however, their lower intrinsic luminosity implies that planets with relatively close-in orbits may have mild equilibrium temperatures and thus be potentially habitable.

According to our current definition, a habitable planet is one that has a surface temperature that allows for the presence of liquid water (i.e.,  $T_{\text{surf}} = 273\text{--}373\text{K}$ ; the existence of a surface implies a planet of terrestrial type). This definition naturally gives rise to the concept of a habitable zone around a star as the range of orbital distances that could sustain liquid water on the surface of a planet (e.g., Kasting et al. 1993, Selsis et al. 2007). As can be seen in Fig. 1, the distance of the habitable zone to the star decreases with decreasing stellar temperature, and therefore stellar mass. As a result, M dwarfs are in the focus of ongoing and planned surveys for habitable planets (see also Tarter et al. 2007, Charbonneau et al. 2009). It is thus clear that a very promising approach is the measurement of precise radial velocities of low-mass stars with the aim of discovering terrestrial-type planets inside the habitable zone. CARMENES will be optimized towards this goal.

## 2. THE SCIENCE CASE FOR CARMENES: TERRESTRIAL PLANETS IN THE HABITABLE ZONES OF M DWARFS

### 2.1 Why M Dwarfs?

The overall aim of CARMENES is to perform high-precision measurements of stellar radial velocities with long-term stability. The fundamental science objective is to carry out a survey of late-type main sequence stars (with special focus on moderately active stars of spectral type M5 and later) with the goal of detecting low-mass planets in their habitable zones. For stars later than M4–M5 ( $M < 0.20 M_\odot$ ), a radial velocity precision of  $1 \text{ m s}^{-1}$  (per measurement;  $\sigma_i$ ) will permit the detection of super-Earths of  $5 M_\oplus$  and smaller inside the entire width of the

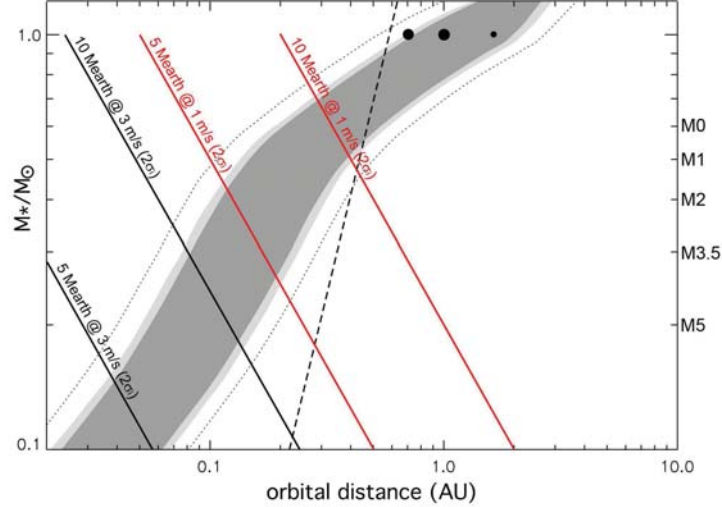


Figure 1. Habitable zone (shaded area) as a function of stellar mass and orbital distance. Approximate stellar spectral types are indicated in the right y-axis for reference. The dashed line indicates the tidal locking distance. Solid lines illustrate the limits for the detection (at the significance of twice the individual measurement error,  $\sigma_i$ ) of super-Earth type planets ( $5 M_{\oplus}$  and  $10 M_{\oplus}$ ) at different radial velocity precisions (1 and  $3 \text{ m s}^{-1}$ ). The accessible regions are to the left of the lines.

habitable zone with  $2\sigma_i$  radial-velocity amplitudes\* (i.e.,  $K_p = 2 \text{ m s}^{-1}$ ). For a star near the hydrogen-burning limit and a precision of  $1 \text{ m s}^{-1}$ , a planet as small as our own Earth in the habitable zone could be detected. In addition, the habitable zones of all M-type dwarfs can be probed for super-Earths. These limits are illustrated in Fig. 1. Thus, to complete the proposed survey, a radial velocity precision (long term) of  $1 \text{ m s}^{-1}$  is required.

Guided by our estimates below (see Sect. 4.1), we plan to survey a sample of 300 M-type stars for low-mass planet companions. This will provide sufficient statistics to assess the overall distribution of planets around M dwarfs: frequency, masses, and orbital parameters. The seemingly low occurrence of Jovian planets should be confirmed, and the frequency of ice giants and terrestrial planets should be established along with their typical separations, eccentricities, multiplicities, and dynamics. The CARMENES sample will be carefully selected to address the distribution of planets in an optimal manner. In this sense, both the detection and non-detection of planets are very relevant results that provide valuable statistical constraints. The CARMENES survey will provide further insight into planet formation and evolution models, which are still largely unconstrained in the case of low-mass planets around low-mass stars.

But additionally, the CARMENES planet search experiment will provide objects that can be further characterized, both their bulk and detailed properties. This is especially tantalizing for low-mass planets in the habitable zone, since observations could determine their nature (ice or telluric). Further, their study can potentially reveal the existence of an atmosphere and, perhaps, determine its chemical composition. The exoplanets from CARMENES will be prime objects for further characterization, via photometric modulation or direct detection, because of their being nearby (the bulk of the target sample is at distances of less than 20 pc). Their study is among the main objectives of several space missions, notably JWST. The habitable planets targeted by CARMENES, i.e., around late M-type dwarfs, have higher chances of undergoing transits than those around Solar-type stars (1.5% vs. 0.5%), and such transits are also deeper (5–15 mmag vs. 0.2 mmag). While there are ongoing photometric M-star transit search experiments (such as MEarth, Irwin et al. 2009), the very nature of targeted surveys implies a limited detection efficiency from a single site. The CARMENES sample of radial velocity planets will permit an efficient search for transiting systems with no time sampling bias. Depending on

\*Note that this is a realistic, and even conservative, detection threshold. Planet detections such as Gl 581 d and Gl 581 e (Mayor et al. 2009b) show that  $\sim 1\sigma_i$  modulations in velocity can have high significance provided that a sufficient number of measurements are obtained.

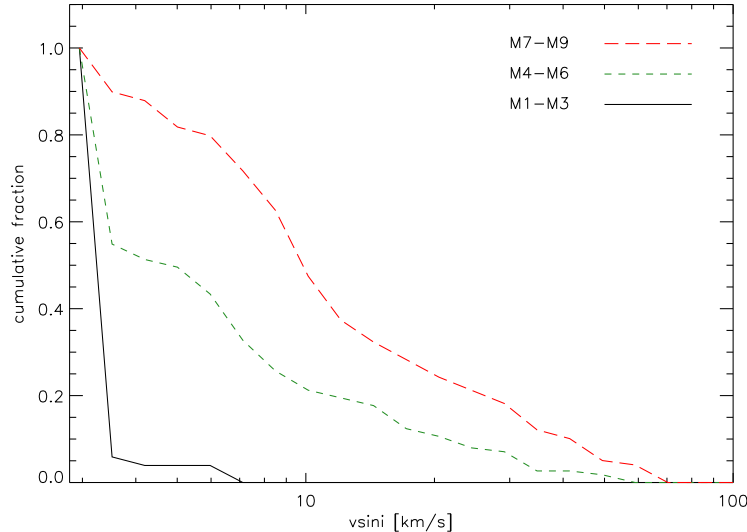


Figure 2. Cumulative plot showing the fraction of early-M (M1–M3), mid-M (M4–M6), and late-M (M7–M9) stars rotating faster than a given value of  $v \sin i$  (from Reiners et al. 2010). For example, about 20% of the M4–M6 stars rotate faster than  $v \sin i = 10 \text{ km s}^{-1}$ .

the abundance of low-mass planets around low-mass stars, several transiting objects should be found within the CARMENES sample of 300 targets.

As an added value, the spectrograph can be used to observe active late-type stars in general to search for small planets since the effects of activity are significantly diminished in the near-IR (see Sect. 2.3). The near-IR spectrograph will be complemented by the visual arm, which will simultaneously monitor the targets for activity-induced variations and avoid false-positive detections, which are a source of major concern. As a bonus, the high-resolution near-IR data will allow us to study the target stars with unprecedented detail, including their full characterization regarding atmospheric parameters and activity, and possibly carry out powerful diagnostics via asteroseismology analyses.

Current planet search experiments in the visible can only probe Solar-type stars and some early M-type stars (typically earlier than M3) with the lowest activity levels. With its combination of near-IR and visible spectrographs, CARMENES will explore the largely uncharted territory of low-mass planets around very late-type stars. This is still a poorly exploited scientific niche with enormous potential that can provide a breakthrough in our knowledge of habitable terrestrial planets; a question of considerable scientific and social interest.

## 2.2 Properties of M Dwarfs

Active regions on stellar surfaces can influence the spectra of stars and are a potential problem for accurate radial velocity measurements. Desort et al. (2007) have shown that spots on Sun-like stars can cause radial velocity variations on the order of  $10\text{--}100 \text{ m s}^{-1}$  depending on the rotation of the star. Similar effects can be expected in M dwarfs. In case of a stable spot or spot configuration, radial velocity variations are synchronized with the rotation period. Thus, it is important to measure the rotation periods/velocities of the stars in order to be able to differentiate between the rotation period of the star and the orbital period of a planet. In M dwarfs, spot lifetimes are probably shorter and spots are more evenly distributed than in Sun-like stars. Thus, differentiation between an orbital period, a rotational period, and the lifetime of spots may not be straightforward.

Active M dwarfs show flares that can potentially affect their spectra, with flare rates of up to several flares per hour. Recently, Reiners (2009) has shown that flaring even in a very active star does not have a strong influence on radial velocity measurements; radial velocity variations are smaller than  $10 \text{ m s}^{-1}$  even during flares as strong as  $\Delta \log(L_{\text{H}\alpha}/L_{\text{bol}}) = 0.4 \text{ dex}$ . This is, however, an order of magnitude above our requirements. For inactive M stars, Zechmeister et al. (2009) found weak correlations between activity and radial velocities on the

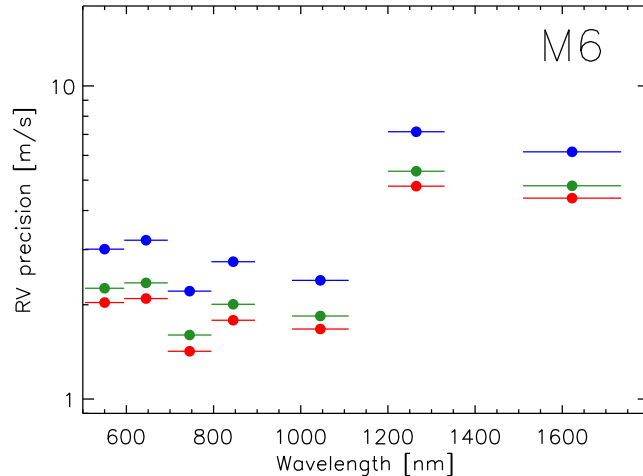


Figure 3. Radial velocity precision for a 2800K star (M6). Simulations are calculated for an SNR of 150 in the  $J$  band at  $R = 85,000$ , and are scaled for three different spectral resolutions assuming identical flux (red:  $R = 100,000$ , green:  $R = 85,000$ , blue:  $R = 60,000$ ). Horizontal lines show the spectral coverage used for the calculation. Filled circles show the best achievable precision, i.e., the intrinsic stellar information content at given data quality.

order of  $2 \text{ m s}^{-1}$  or below in a small number of targets. At the  $1 \text{ m s}^{-1}$  level, we clearly have to take into account activity effects, which requires broad wavelength coverage including the near-IR range.

Many late M dwarfs are rapid rotators, with a tendency of cooler M dwarfs (later than M3) to rotate more rapidly than the earlier sub-types. The precision of radial velocity determinations is lower in the presence of rotation. At lower mass, hence generally faster rotation, there is thus a trade-off between lower radial velocity precision (because of higher  $v \sin i$ ) and higher semi-amplitude (because of lower stellar mass). The CARMENES consortium is participating in an ongoing effort to measure  $v \sin i$  in several hundred early M dwarfs that can be used for the target list. At this point, it is clear that slow rotators do exist — and hence can be selected for our sample — even among the late-M dwarfs (see Fig. 2). Thus, the best possible RV precision directly translates into the lowest detectable planetary mass even at the latest spectral types in our sample.

### 2.3 Scientific Requirements

Stars less massive than  $M = 0.3 M_{\odot}$  have temperatures lower than  $T \approx 3000 \text{ K}$  and emit the bulk of their flux at infrared wavelengths. Although a number of planets around early-M dwarfs were found with visible spectrographs, mid- and late-M dwarfs are too faint in this wavelength range to reach the data quality required for the detection of planets. Redward of  $\sim 1 \mu\text{m}$ , the flux emitted by these stars is several factors higher so that at NIR wavelengths, many low-mass stars are in principle bright enough to be observed at very high precision.

The precision achievable with the radial velocity technique depends on the following factors:

- Signal-to-noise ratio (SNR) of the spectrum;
- Wavelength coverage;
- Occurrence and shape of spectral lines (sharp and deep lines required);
- Stability of the spectrograph and the wavelength calibration;
- Stellar factors (activity, rotation, etc.).

Table 1. RV precision per wavelength bin for different spectral types. The rightmost column shows the final RV precision achievable if all wavelength bins are combined. The spectral resolution of CARMENES is planned to be  $R = 85,000$ .

Resolution	RV precision ( $\text{m s}^{-1}$ )							
	$\lambda_{\text{start}} = 500 \text{ nm}$	600	700	800	980	1200	1510	<b>500–1350</b>
	$\lambda_{\text{end}} = 600 \text{ nm}$	700	800	900	1110	1330	1735	<b>combined</b>
Spectral Type M3								
60000	2.0	2.2	2.7	4.7	3.2	12.9	5.6	1.2
<b>85000</b>	1.5	1.7	1.9	3.6	2.4	9.8	4.6	<b>0.9</b>
100000	1.4	1.5	1.7	3.3	2.1	8.8	4.3	0.8
Spectral Type M6								
60000	3.0	3.2	2.2	2.7	2.4	7.1	6.2	1.2
<b>85000</b>	2.3	2.3	1.6	2.0	1.8	5.3	4.8	<b>0.9</b>
100000	2.0	2.1	1.4	1.8	1.7	4.8	4.4	0.8
Spectral Type M9								
60000	6.0	6.0	2.6	2.4	1.7	3.5	3.0	1.1
<b>85000</b>	4.4	4.3	1.9	1.7	1.2	2.5	2.6	<b>0.8</b>
100000	4.0	3.8	1.7	1.5	1.1	2.2	2.5	0.7

In order to identify the wavelength range that is most suitable for the search for radial velocity variations in low-mass stars, we have carried out detailed simulations of the achievable precision of such a measurement (see also Reiners et al. 2010). In our simulations, we take into account the flux distribution of the star, the occurrence and shape of spectral features, the wavelength coverage of a given spectrograph, and the precision of the wavelength calibration strategy. Our simulations put our considerations of the optical layout of the near-IR and visible spectrograph on firm ground. As an example, we show in Fig. 3 the results for an M6 star observed at different wavelengths, namely in the visible and near-IR bands from  $V$  to  $H$ .

For our simulations, we calculated the intrinsic precision over the wavelength bin under consideration. For Fig. 3, we assume an SNR of 150 in the  $J$  band at  $R = 85,000$ , which is the minimum SNR requirement for our faintest targets. We scale the signal quality according to the spectral flux distribution and spectral resolution assuming constant flux and instrument efficiency (note that higher precision can always be achieved with higher SNR), and calculate the achievable precision for several configurations. No rotational broadening is applied to the model spectra. The question Fig. 3 tries to answer is what is the highest attainable precision of a radial velocity measurement if a given star is observed at different wavelength regions and spectral resolutions, under the assumption of the same exposure time, telescope size, and instrument throughput for all setups.

In Sun-like stars (not considered further here), the visible band is the most suitable wavelength range for radial velocity measurements. For an early-M star (M3), the  $R$  and  $I$  bands are still slightly better than the  $Y$  band (starting at  $\sim 1000 \text{ nm}$ ), but by a small margin. The situation reverses at spectral type M6 and later, where particularly the  $Y$  band becomes clearly better than the visible band. The  $J$  and the  $H$  bands are about a factor of two worse. For spectral types as late as M9, the highest obtainable precision (per exposure) in the  $Y$  band at  $R = 85,000$  is well below  $2 \text{ m s}^{-1}$ ; in the  $J$  and  $H$  bands, it is a factor of two worse. At this low effective temperature, the difference in flux shows a striking effect on the obtainable precision. Since the main focus of our project are stars of spectral type later than M5, there is a clear advantage of a spectrograph covering the wavelength range redward of  $700 \text{ nm}$ , and in particular the  $Y$  band from  $950 \text{ nm}$  upwards.

We summarize the anticipated RV precisions per wavelength range for spectral types M3, M6, and M9 in Tab. 1. The RV precisions calculated include the design of the CARMENES observations, i.e.,  $R = 85,000$  and  $\text{SNR} = 150$  at  $J$  (green symbols in Fig. 3), the other setups are scaled conserving flux. The highest possible RV precision will be reached by adding all information coming from different bands. For highest RV precision, we plan to combine the spectral information up to  $1.35 \mu\text{m}$ . The combined RV precision is also given in Tab. 1. Our calculations show that a SNR in excess of 150 in the  $J$  band will provide enough spectral information to reach the required radial velocity precision goal of  $1 \text{ m s}^{-1}$  among all spectral types.

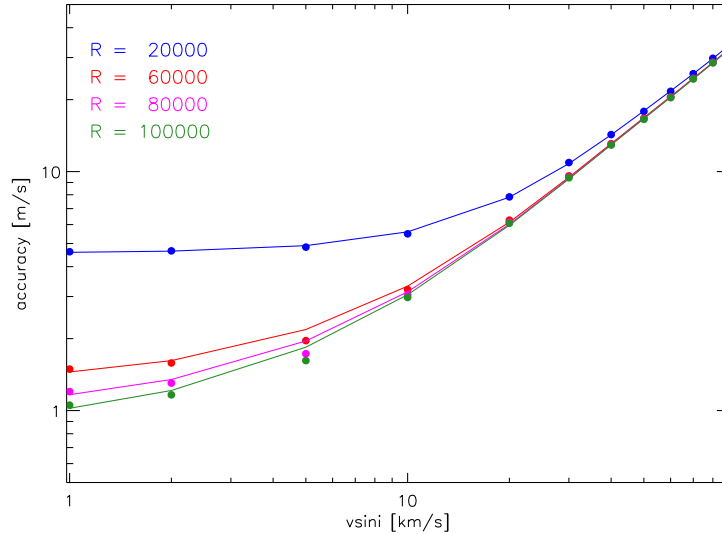


Figure 4. Simulation of radial velocity precision for different spectrograph resolutions and stellar rotational velocities.

Thus, the minimum wavelength range required to achieve the goals of our survey is  $\sim 600$  nm to  $\sim 1.2$   $\mu\text{m}$ . However, there are a few additional considerations worth taking into account. Firstly, the effects of activity jitter will be diminished in the *J* and *H* bands compared with *Y*, but by a relatively small margin (*H* band jitter being lower by 20–30% compared with the *Y* band), as discussed below. The *Y* band itself seems to provide an important step in jitter reduction and hence is required for spot-planet discrimination, too. Secondly, all calculations depend on the assumed synthetic spectra because so far no high-quality observed spectra across the M spectral regime are available. The models we used are state-of-the-art models, but still with the intrinsic limitations coming from an imperfect knowledge of molecular transitions (both abundance and strength). Based on the model improvements made during the past years and on previous experience, we do not expect our precision calculations to be off from reality by more than a factor of two, either way (i.e., improving or worsening the estimates), but there is some room for refinement in particular among the relative results of RV accuracies. In fact, CARMENES will be the first spectrograph providing data of this quality in the near-IR.

For late-M spectral types, the wavelength range around  $1$   $\mu\text{m}$  (*Y* band) is the most important wavelength region for radial velocity work. Therefore, we must make every effort to optimize the instruments efficiency in this range. Unfortunately, CCDs do not provide high enough efficiency around  $1$   $\mu\text{m}$  and no signal at all beyond the Si cutoff at  $1.1$   $\mu\text{m}$ . Thus, a near-IR detector is required.

In summary, a near-IR spectrograph will provide radial velocities of unsurpassed precision for stars of spectral type M6 and later. The *Y* band delivers the best precision but the *J* and *H* bands should also be considered to allow for proper estimate of activity effects and for a potential contribution to improving the *Y*-band velocity estimate by some 30–40%. Thus, the required wavelength coverage for the near-IR spectrograph is  $0.95$ – $1.35$   $\mu\text{m}$ . Our design allows for larger red coverage up to  $1.7$   $\mu\text{m}$ , but we will focus on optimizing the range  $0.95$ – $1.35$   $\mu\text{m}$ , which is the most valuable scientifically.

We have carried out detailed simulations of radial velocity jitter in preparation for our M dwarf planet search. Since activity is believed to be one of the most challenging problems mimicking radial velocity variations or making radial velocity signals invisible, and because of the dependence of the activity signal on the wavelength regime, we calculated the radial velocity signal of a co-rotating spot as a function of wavelength in different stellar environments (Reiners et al. 2010). Our simulations show that the radial velocity signal is wavelength dependent, and that the amplitude of the wavelength dependence is a function of effective temperature and of the temperature difference between the spot and the surrounding photosphere. Thus, not only can activity-induced radial velocity variations be distinguished from real motion due to a planet, the wavelength dependence of jitter also provides tight constraints on the properties of the surface features. The largest reduction of jitter occurs at

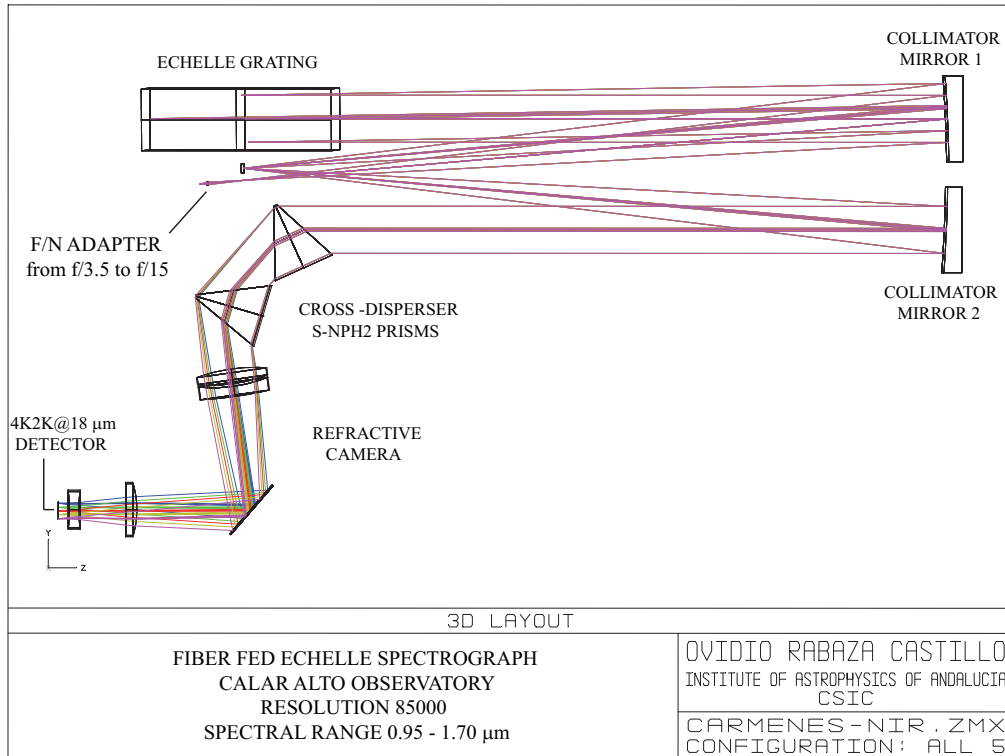


Figure 5. Layout of the NIR channel optical design.

the lowest temperatures and if the contrast between the spots and the surface is relatively small (a few hundred kelvins).

The concept of a dual-channel spectrograph will permit the determination of radial velocity variations at different wavelengths simultaneously. Activity-induced velocity variations are expected to be wavelength dependent, which is strictly not the case for orbital variations. Thus, it will be possible to differentiate an orbital period from activity, and the wavelength dependence will provide valuable information on the spot temperature and distribution.

To take full advantage of the information content in a stellar spectrum for radial velocity measurements, the spectrograph resolution has to be matched to the stellar line width. Since many of the potential targets for CARMENES have rotational velocities of  $3 \text{ km s}^{-1}$  or less, a resolution of up to  $\sim 100,000$  could be usefully exploited. As a compromise between cost, size, and complexity on one hand, and performance on the other hand, the CARMENES spectrographs will have  $R \sim 85,000$ .

### 3. INSTRUMENT DESIGN

#### 3.1 Near-Infrared Spectrograph

The conceptual design of the CARMENES near-IR spectrograph is based on a bench-mounted echelle spectrograph that receives light from the 3.5 m telescope through a set of optical fibers. Fiber-fed systems allow the spectrograph to be mounted in an isolated chamber, improving the thermal and mechanical stability, and provide basic scrambling of the spatial information of the image on the input end of the fiber, thus smoothing out seeing and guiding variations.

As in many other modern high-resolution spectrographs, the optical design of CARMENES-NIR is based on a white pupil layout (see Fig. 5). This is one of the best solutions for a high-resolution instrument that has to operate over a wide wavelength range. The white pupil layout offers several advantages over most of the spectrograph mountings:

<b>NIR Spectrograph, two 2k×2k detectors</b>	
<b>Optical design</b>	fiber-fed, cross-dispersed echelle spectrograph
<b>Number of fibers (science+calibration)</b>	2
<b>Fiber aperture on sky</b>	1.65'' = 100 μm
<b>Slit aperture</b>	0.55''
<b>EFFL Collimators</b>	1483.4 mm
<b>Collimated beam diameter</b>	100 mm
<b>Covered spectral range</b>	950 nm to 1700 nm
<b>Echelle grating</b>	R4@31.6 lines/mm
<b>Cross-disperser</b>	2 S-NPH2 prisms
<b>Camera field radius in dispersion direction</b>	±3.69°
<b>EFFL Camera</b>	572.2 mm
<b>Spectral resolution</b>	$R = 85,000$
<b>Spectral format</b>	30 echelle orders 73.73 × 36.86 mm
<b>Detector format</b>	Mosaic of two 2k×2k detectors; pixel size = 18 μm
<b>Sampling</b>	3 pixels

Table 2. NIR-spectrograph parameters for mosaic detector.

- The control over the second pupil avoids vignetting in the spectrograph.
- The echelle grating can be mounted easily in a quasi-Littrow configuration. In this layout, the luminosity × resolution product, an important figure of merit for spectrograph performance, is at its maximum.
- The collimator focal length is a free parameter, offering extra flexibility.
- As the camera does not directly “see” the echelle grating, stray light contamination is low. Moreover, it can be further reduced by installing a field stop at the position of the intermediate spectrum in the vicinity of the slit, as well as by inserting dedicated baffles on the optical bench.

Obtaining a very high efficiency has been a mayor driver throughout the complete instrument design phase, as well as in the selection of the different components. With the current conceptual design, CARMENES-NIR will cover a wide spectral range (950 to 1700 nm in 30 orders) in an efficient way and in a single exposure on the detector. This wide spectral range also allows for a completely fixed spectrograph configuration, which again improves the instrumental stability. The main parameters of the spectrograph design are summarized in Tab. 2.

The camera is a fully dioptric system that consists of four lenses. It has a focal length of 572.2 mm and a geometric focal ratio of  $f/5.8$ . The camera covers a circular field of  $\pm 4.12^\circ$  and has a clear entrance aperture of 130 mm. At  $\lambda = 1 \mu\text{m}$ , the estimated efficiency of the camera is 85%. The baseline foresees a mosaic of two  $2\text{k} \times 2\text{k}$  pixel Hawaii-2RG detectors optimized for the 0.8 to 1.7  $\mu\text{m}$  wavelength range.

The near-IR spectrograph will be bench-mounted and placed inside a vacuum tank housing. Most optical subsystems (focal adapter, image slicer, off-axis parabolic mirrors, echelle grating, flat mirrors, cross-disperser prisms, refractive camera and exposure meter) and their holders will be mounted inside the vacuum tank. The detector will not be placed inside the vacuum tank to facilitate handling, AIV and maintenance. Therefore there will be a separate detector dewar for the near-IR detector, which will be attached to the vacuum tank by means of vacuum-compatible hardware.

The vacuum tank will be cooled to an operational temperature of  $-30^\circ\text{C}$  ( $\sim 243\text{K}$ ) with a stability of  $\pm 0.01^\circ\text{C}$ . Since the working temperature is not far below the ambient temperature, the solution chosen to properly cool down the instrument is based on thermal conditioning of the environment by means of three embedded environment-controlled rooms, one inside another.

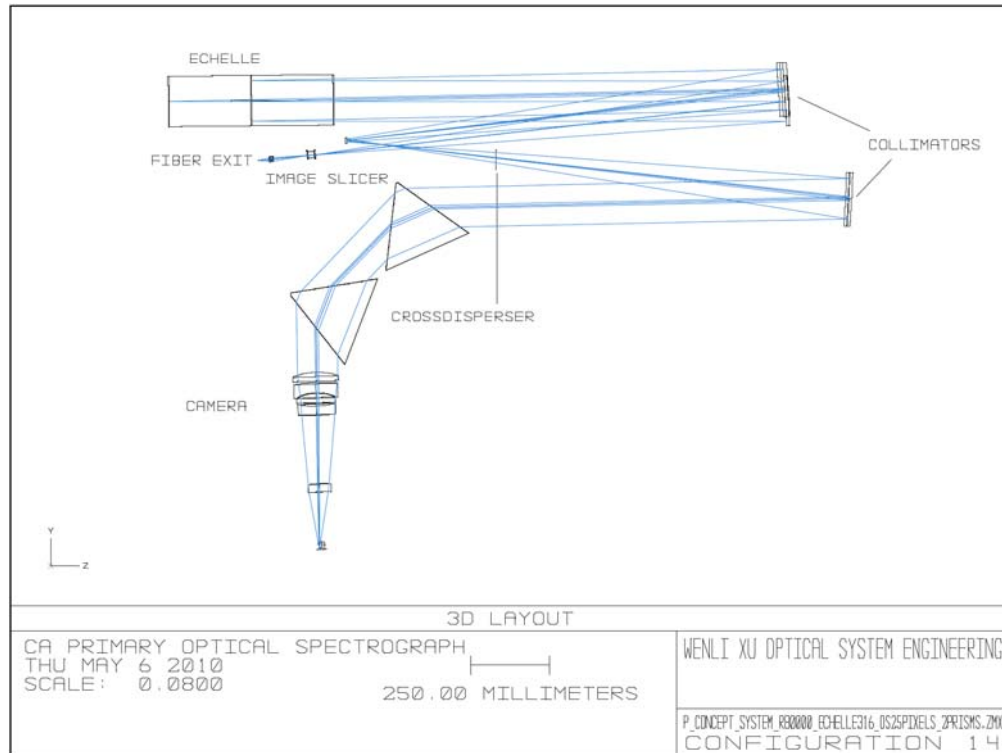


Figure 6. Basic layout of the optical spectrograph.

### 3.2 Visible-Light Spectrograph

The optical spectrograph is also a bench-mounted white pupil design (Fig. 6); it is based on the design of the FEROS spectrograph now at the ESO 2.2 m telescope. The light exiting the fiber is converted by a lens system to a focal ratio appropriate for the spectrograph collimator. After a two-slice image slicer, the entrance “slit” is formed. The main collimator is an off-axis paraboloid; it collimates the light onto the mosaic echelle grating. The proposed mosaic echelle grating is an R4 with 31.6 lines per millimeter. The dispersed back reflection under a small angle goes back to the main collimator and then, after folding of the light path by a small flat mirror near the entrance slit, arrives at the second transfer collimator. This produces a pupil close to the front surface of the cross disperser. Here, stray light can be filtered out effectively. Cross dispersion is done by a prism in order to reach high efficiency over the complete wavelength range. The dioptric camera has a focal length of 408 mm, and a focal ratio of  $f/3.2$ . The detector foreseen is an e2v  $2048 \times 4096$  CCD. The main parameters of the optical spectrograph are summarized in Tab. 3.

The optical spectrograph is designed for a detector with  $2k \times 4k$  pixels, with a pixel size of  $15 \mu$ . Only a few detectors with these specifications are available. We have foreseen as a baseline the e2v detector CCD44-82, since it is available as a “deep-depletion” variant, which suppresses fringing, which is a strong concern in the red spectral range. In addition, this detector can be coated in a position dependent form (“graded coating”), such that the efficiency is maximum for each position in cross-dispersion direction.

The optical spectrograph will also be operated in vacuum and stabilized to  $\pm 0.01^\circ\text{C}$ , but it will be operated near or slightly below room temperature.

### 3.3 Radial-Velocity Calibration

Because there is currently no known gas cell that gives a sufficiently dense grid of absorption lines over the whole bands used by CARMENES, the ThAr method has been adopted as a baseline for the precise wavelength

Wavelength range	0.523–1.05 $\mu\text{m}$ (59 orders)
Spectral resolution	80 000 (with two-slice image slicer)
Spectrograph	
Entrance aperture	1.5''
Fiber input focal ratio	$f/3.93$
Fiber output focal ratio	$f/3.5$
Spectrograph beam size	127 mm
Off-axis collimators	$f/11.8$ (cut from one parent paraboloid)
Echelle grating	R4 (76°), 31.61 mm <sup>-1</sup> , 127 mm × 508 mm
Cross disperser	2 prisms, glass LF5, apex angle 61°
Refractive camera	
Focal ratio	$f/3.2$
Focal length	408 mm
Sampling	2.7 pixels
Detector	2048 × 4096 CCD, 15 $\mu\text{m}$ /pixel

Table 3. Basic optical parameters of the VIS channel.

calibration. A stabilized etalon is currently under investigation as a potential alternative. The system is flexible enough so that light from an etalon can easily be fed through the calibration fiber instead of the ThAr lamp.

For the ThAr method it is required that the drift between the spectra of the star and of the lamp during a night is smaller than the desired accuracy of the RV measurements, i.e. 1 m/s in the case of CARMENES. In order to minimize the drift between the two spectra, the light of the star and the light of the calibration lamp are fed into the spectrograph via fibers. For each spectrograph, two fibers are used: one for the star light, the other for the ThAr lamp. Since the exposure times for the lamp and the star are identical, a filter of variable transmission is needed for dimming down the ThAr lamp during a long exposure. To avoid that tracking errors of the telescope induce shifts of the spectrum on the detector, instruments like HARPS use double image scramblers in addition to fibers. We will follow a similar procedure for CARMENES; methods to perform the scrambling with maximum throughput are currently under investigation.

Some important issues to be addressed by the design of the calibration system are:

- *Number of spectral lines per wavelength interval.* RV measurements are essentially measurements of the position of lines on the detector. This means that it must be possible to measure the “astrometric” distortion on the detector with sufficient accuracy with the number of lines available. The atlas by Kerber et al. (2008) lists about 1500 ThAr lines in the complete wavelength regime of CARMENES up to 1.8  $\mu\text{m}$ . With an appropriate optical design, this number of lines is sufficient for achieving an accuracy of 1 m/s.
- *Ageing effects of the ThAr lamps.* Changes of the pressure inside the lamp when it gets older cause changes of the spectrum of the lamp, which in turn lead to errors in the wavelength calibration. This effect is far more significant for argon lines than thorium lines. This differential effect can be used to correct for the lamp ageing effect (Mayor et al. 2009a). Additionally, at least two ThAr lamps, which can quickly be exchanged, will be installed. One or more lamps will be used for the nightly observations (slave lamps), the other one (master lamp) only rarely in order to monitor the changes of the slave lamps (the master lamp will have a longer lifetime because it is used less frequently).
- *Cross-talk between the fibers.* In the case of HARPS, the stability is so good that the simultaneous wavelength calibration is often not used during the night; ThAr spectra are only taken at the beginning and at the end of the night. In this way, the problem of the cross-talk of the fibers is completely avoided. In any case, the cross-talk between the fibers has to be minimized.

Exposure meters are necessary to continuously record the flux that enters the two spectrographs, in order to compute the true (i.e., photon-weighted) mean time of the exposure, which is critical for an accurate correction of

the observed radial velocity to the barycenter of the Solar System. In order to avoid removing any flux from the science beam, the exposure meters will obtain the flux from the zeroth diffraction order from the echelle gratings, which will be collected with a mirror and focused on a photo-multiplier. As a fringe benefit, this information is very helpful in setting the optimum exposure time of targets of different apparent magnitudes and colors, especially under non-photometric observing conditions.

## 4. SURVEY OPERATIONS

### 4.1 Survey Strategy

The CARMENES low-mass planet search will concentrate on a sample of very late-type M dwarfs. Monitoring in the visible at high precision with the HARPS instrument has shown that there is a trend of increasing planet occurrence with decreasing planet mass around M-type stars. Statistics indicate that, while Jupiter-like planets occur in about 10% of the stars, Neptune- and lower-mass planets (at least in close-in orbits) seem to be present in about 30% of the monitored stars (Mayor et al. 2009a). The same trend is found in the extensive Kepler planet search, where super-Earth and Neptune-type candidates are found to be relatively more abundant than Jupiter candidates as the host stellar mass decreases (Borucki et al. 2010). Therefore, it is possible that low-mass planets are very abundant around M dwarfs.

Our survey strategy is to intensively monitor a well-characterized sample of about 300 M dwarfs. We can estimate the percentage of stars with low-mass planets from current results of planet surveys and modeling. About 5% of the Solar-mass stars harbor gas giants. Earth-mass planets can be expected to be much more frequent (e.g., Mordasini et al. 2009a). If we assume that about 30% of the M dwarfs have low-mass planets and a high chance of some being in the habitable zone, we may expect to find between 50 and 100 suitable planets. Note that this estimate is obviously rather vague, but even if the real frequency of planets is much lower, still a substantial number of suitable planets is available, and our project will put tight constraints on the fraction of low-mass planets.

The expected CARMENES planet harvest is, at any rate, sufficient to carry out a reliable statistical analysis of the planet population and shed light on the architecture of planetary systems and on the formation mechanisms. For example, Mordasini et al. (2009b) carried out a meaningful comparison with model predictions (including migration and other processes) with a sample of 32 exoplanets. The CARMENES survey will also provide valuable constraints on the much-sought value of the  $\eta_{\oplus}$  parameter for M-dwarfs, which is the frequency of terrestrial planets in the habitable zone. Given the transit probability and the favorable selection bias, there is also a good chance that 1 or 2 transiting planets will be amongst these CARMENES discoveries. These hold such extraordinary value for future investigations that their discovery merits all efforts.

Given a final target sample of 300 objects, we will necessarily have to start with a larger list of some 400 to 450 stars from which we will drop those that are not suitable for high precision radial velocity work (fast rotators, close binaries, very active stars) after taking a few measurements ( $\sim 5-10$ ). For the working sample of 300 stars we plan to obtain at least 60 measurements per object and we will go up to 100 measurements or more for the most interesting systems. The experience gathered with observations in the visible indicates that exoplanets can already be identified with about 30 measurements, although  $\sim 100$  measurements per object are needed for the detection of a planet with radial velocity semi-amplitude close to the measurement error (e.g., Udry et al. 2007, Mayor et al. 2009a, 2009b). In this scheme, the total number of measurements needed to achieve the goals of our project is:

- 3,500 measurements for sample clean-up (510 measurements per object);
- 15,000 additional measurements for 300 targets (for a total of 60 measurements each);
- 4,000 additional measurements for 100 targets (for a total of 100 measurements each).

This yields a grand total of 22,500 measurements.

To observe the sample we will use a typical integration time of 900s to avoid blurring of the stellar lines because of the Earth's diurnal motion. When considering the expected instrument overheads this leads to an

estimate of some 3 measurements per hour or some 25 measurements per night. Assuming 180 nights per year, this implies roughly 4,500 measurements per year and 22,500 measurements over the course of 5 years. The calculations indicate that, with some further optimization, the goals of the project can be attained with intensive (perhaps exclusive) use of the instrument at the 3.5 m telescope during 5 years.

The timing of the observations will be selected to sample adequately the relevant periods (i.e., low-mass planets with particular attention to those orbiting in the habitable zone). Also, and especially at the start of the program, we will collect radial velocity time series with high cadence to investigate the pulsation properties of M stars, which are still largely unknown. This will help to optimize the integration time for planet searches so that pulsation modes can be averaged out, as routinely done for Solar-type stars in the visible. In any case, current experience from HARPS in the case of M type stars (e.g., the M3 star Gl 581, Mayor et al. 2009b) shows that intrinsic pulsations will not be a limiting factor to reach the  $1 \text{ m s}^{-1}$  precision level.

## 4.2 Data Reduction

The main purpose of CARMENES is to provide high-precision differential radial velocities. Full analysis of the data obtained by the spectrograph implies two steps: (1) classical data reduction from raw 2D frames to wavelength-calibrated 1D spectra, and (2) measurement of radial velocities. For optimizing the scientific output of the instrument, it is essential to have software that delivers reduced spectra and measured velocities at the telescope, and also allows efficient re-processing of all existing data as analysis methods are refined.

The data analysis software will be supplied by the CARMENES Consortium and will be implemented in a pipeline fashion to minimize interaction with the user. The two parts will be implemented separately for the NIR and VIS channels based on the same software packages. Since the strategies for wavelength calibration and radial velocity analysis are essentially identical in the VIS and NIR arms, large parts of the software packages can be shared. The software modules for each part and arm will be developed in one consistent software package that will be installed at Calar Alto and at the institutes in charge of data reduction. The pipeline will allow a first run of the data reduction during the night to constantly monitor integrity and data quality. This will allow immediate response to changing weather conditions and to quick identification of problems. During the next day, science quality data reduction and radial velocity measurements will be performed after all calibration exposures are taken.

The final calibration and data reduction strategy will be subject to refinement during the time of operation. Effects like dark current, non-linearity, and the influence of calibration lamp degradation will have to be carefully investigated during and after the commissioning phase. For example, although the spectrum of ThAr is well documented, individual lamps deliver spectra that are slightly different, and the quality of individual lines will have to be checked. Therefore, the bulk of the calibration plan will be finalized during the phase of commissioning, but it will probably be subject to improvement as the instrument and software become more and more mature.

Constant refinement of the reduction and analysis procedures means that a complete and consistent re-reduction of the full data set will need to be performed when a new software version becomes available. This will be carried out at the institutions in charge. The baseline calibration method is using emission lines from a ThAr lamp. It is foreseen that more stable calibration sources will become available before or during the operation of CARMENES. All options under consideration deliver light in the form of emission lines that can be used in strict analogy to the ThAr lines. An exchange of the calibration line source would obviously mean a modification to the data reduction software, but the basic strategy remains the same. Therefore, such a modification of CARMENES is not expected to lead to any problems with data reduction and analysis.

## ACKNOWLEDGMENTS

The CARMENES concept study was funded by the Centro Astronómico Hispano-Alemán, which is operated jointly by the Max-Planck-Institut für Astronomie (Max-Planck-Gesellschaft) and the Instituto de Astrofísica de Andalucía (Consejo Superior de Investigaciones Científicas). PJA acknowledges financial support from a “Ramon y Cajal” contract of the Spanish Ministry of Education and Science.

## REFERENCES

- [1] Borucki, W.J., Koch, D.G., Basri, G., Batalha, N., Brown, T. et al. (2010). *Characteristics of Kepler planetary candidates based on the first data set: the majority are found to be Neptune-size and smaller*. ApJ, submitted (astro-ph 1006.2799)
- [2] Charbonneau, D., Berta, Z.K., Irwin, J., Burke, C.J., Nutzman, P., et al. (2009). *A super-Earth transiting a nearby low-mass star*. Nature 462, 891-894
- [3] Desort, M., Lagrange, A.M., Galland, F., Udry, S., & Mayor, M. (2007). *Search for exoplanets with the radial-velocity technique: quantitative diagnostics of stellar activity*. A&A 473, 983-993
- [4] Irwin, J., Charbonneau, D., Nutzman, P., & Falco, E. (2009). *The M<sub>Earth</sub> project: searching for transiting habitable super-Earths around nearby M dwarfs*. In *Transiting Planets*, Proc. IAU Symp. 253, 37-43
- [5] Kasting, J.F., Whitmire, D.P., & Reynolds, R.T. (1993). *Habitable zones around main sequence stars*. Icarus 101, 108-128
- [6] Kerber, F., Nave, G., & Sansonetti, C.J. (2008). *The spectrum of Th-Ar hollow cathode lamps in the 691-5804 nm region: establishing wavelength standards for the calibration of infrared spectrographs*. ApJS 178, 374-381
- [7] Knutson, H.A., Charbonneau, D., Allen, L.E., Fortney, J.J., Agol, E., et al. (2007). *A map of the day-night contrast of the extrasolar planet HD 189733 b*. Nature 447, 183-186
- [8] Lovis, C., Mayor, M., Pepe, F., Alibert, Y., Benz, W., et al. (2006). *An extrasolar planetary system with three Neptune-mass planets*. Nature 441, 305-309
- [9] Mayor, M., & Queloz, D. (1995). *A Jupiter-mass companion to a solar-type star*. Nature 378, 355-359
- [10] Mayor, M., & Udry, S. (2008). *The quest for very low-mass planets*. Physica Scripta 014010, 1-8
- [11] Mayor, M., Udry, S., Lovis, C., Pepe, F., Queloz, D., et al. (2009a). *The HARPS search for Southern extra-solar planets. XIII. A planetary system with 3 super-Earths (4.2, 6.9, and 9.2 M<sub>⊕</sub>)*. A&A 493, 639-644
- [12] Mayor, M., Bonfils, X., Forveille, T., Delfosse, X., Udry, S., et al. (2009b). *The HARPS search for Southern extra-solar planets. XVIII. An Earth-mass planet in the GJ 581 planetary system*. A&A 507, 487-494
- [13] Mordasini, C., Alibert, Y., & Benz, W. (2009a). *Extrasolar planet population synthesis. I. Method, formation tracks, and mass-distance distribution*. A&A 501, 1139-1160
- [14] Mordasini, C., Alibert, Y., Benz, W., & Naef, D. (2009b). *Extrasolar planet population synthesis. II. Statistical comparison with observations*. A&A 501, 1161-1184
- [15] Reiners, A. (2009). *Activity-induced radial velocity jitter in a flaring M dwarf*. A&A 498, 853-861
- [16] Reiners, A., Bean, J.L., Huber, K.F., Dreizler, S., Seifahrt, A., & Czesla, S. (2010). *Detecting planets around very low mass stars with the radial velocity method*. ApJ 710, 432-443
- [17] Selsis, F., Kasting, J.F., Levrard, B., Paillet, J., Ribas, I., & Delfosse, X. (2007). *Habitable planets around the star Gliese 581?* A&A 476, 1373-1387
- [18] Swain, M.R., Vasisht, G., & Tinetti, G. (2008). *The presence of methane in the atmosphere of an extrasolar planet*. Nature 452, 329-331
- [19] Tarter, J.C., Backus, P.R., Mancinelli, R.L., Aurnou, J.M., Backman, D.E., et al. (2007). *A Reappraisal of the habitability of planets around M dwarf stars*. Astrobiology 7, 30-65
- [20] Tinetti, G., Vidal-Madjar, A., Liang, M.C., Beaulieu, J.P., Yung, Y., et al. (2007). *Water vapour in the atmosphere of a transiting extrasolar planet*. Nature 448, 169-171
- [21] Udry, S., Bonfils, X., Delfosse, X., Forveille, T., Mayor, M., et al. (2007). *The HARPS search for Southern extra-solar planets. XI. Super-Earths (5 and 8 M<sub>⊕</sub>) in a 3-planet system*. A&A 469, L43-L47
- [22] Zechmeister, M., Kürster, M., & Endl, M. (2009). *The M dwarf planet search programme at the ESO VLT + UVES. A search for terrestrial planets in the habitable zone of M dwarfs*. A&A 505, 859-871